Journal of Materials Chemistry C

RSC Publishing

PAPER

View Article Online
View Journal

Cite this: DOI: 10.1039/c3tc31620c

Optically functional surface structures for GaN-based light-emitting diodes

Ming Ma,*[a] Jaehee Cho,*[ab] E. Fred Schubert,[a] Gi Bum Kim[c] and Cheolsoo Sone[c]

Received 16th August 2013
Accepted 17th October 2013

DOI: 10.1039/c3tc31620c

www.rsc.org/MaterialsC

The unrestricted control of the surface structure and refractive index would allow for new and improved functionalities in optoelectronic devices. Specifically, micro-patterned graded-refractive-index (GRIN) coatings can enable control of emission pattern and promote light extraction in GaInN light-emitting diodes (LEDs). We design and demonstrate coatings that are patterned into arrays of GRIN micro-pillars, each composed of five dielectric layers of $(TiO_2)_x(SiO_2)_{1-x}$ with the bottom layer (adjacent to semiconductor) having the highest refractive index and the top layer (adjacent to air) having the lowest one. The GRIN micro-pillars, including their planar geometric shape and size, are structured for emission pattern control and maximum light-extraction efficiency. It is shown that the peak emission intensity of the GRIN LEDs is controllable from $\pm 20^\circ$ to $\pm 50^\circ$ off the surface-normal. In addition, LEDs patterned with an array of four-pointed-star-shaped GRIN micro-pillars with a pillar-size of 4 μm and spacing between neighboring pillars of 4 μm show a 155% enhancement in light-output power over an uncoated planar reference LED.

1. Introduction

Light-emitting diodes (LEDs) are the next-generation lighting source due to their high efficiency, high reliability, and potential to offer new functionalities such as controllable emission patterns.[1–3] It is known that the large refractive-index contrast between the LED semiconductor ($n = 2.5$ to 3.5) and air ($n = 1$) affects the emission pattern of the LED,[4,5] and, at the same time, limits the light-extraction efficiency (LEE) of the LED due to the occurrence of total internal reflection (TIR) at the interface between the LED semiconductor and air.[6,7] As a result, planar-surface LEDs have two limitations: (i) an (uncontrollable) Lambertian emission pattern with the peak emission intensity along the LED surface-normal and a decreasing intensity off the surface-normal, which is not optimized for uniform illumination;[8] and (ii) a very low LEE.[9]

Currently these two limitations are solved separately: (i) the emission pattern of the LED is controlled by secondary optics such as freeform lenses,[10–12] (ii) the LEE of GaN-based LEDs is enhanced by roughening the nitrogen-face GaN surface using crystallographic wet chemical etching.[13–15] However, since both limitations originate from the large refractive-index contrast between the LED semiconductor and air, overcoming both limitations will require advanced and detailed control of both the refractive index and its spatial distribution (*i.e.*, surface structure); such a pervasive control is currently lacking. Given these limitations, the unrestricted control of the refractive index and surface structure would be highly desirable for new and improved functionalities in optoelectronic devices.

The ultimate goal is a surface with unrestricted surface structure and refractive index, *i.e.*, a surface having the surface structure with near arbitrary shape while simultaneously attaining an unrestricted refractive-index profile. For example, such a surface may have tips and trenches, or mountains and valleys, with each individual feature having a well-controlled refractive-index profile. Such optically functional surfaces can open the door to a new degree of control and performance in optoelectronic devices.

As a proof of concept, here we present a technique that provides advanced control of the refractive index and surface structure at the LED surface: LEDs having patterned graded-refractive-index (GRIN) coatings. It will be shown that patterned GRIN coatings can make the surface of an LED chip optically functional, *i.e.*, they can function to (i) increase the light emission in desired directions and thus control the emission pattern of the LED; and (ii) eliminate total-internal-reflection inside the LED semiconductor and hence enhance the LEE of the LED.

Fig. 1a shows the schematic diagram of a GRIN LED with an array of four-pointed-star-shaped GRIN micro-pillars. Each GRIN micro-pillar has a well-defined planar geometric shape, and is composed of five layers of $(TiO_2)_x(SiO_2)_{1-x}$ with varying compositions and thus, refractive indices. The refractive index decreases from the bottom layer, which is refractive-index-matched to the GaN layer to minimize coupling loss, towards the top layer, as

[a]Department of Electrical, Computer, and Systems Engineering, Rensselaer Polytechnic Institute, 110 Eighth Street, Troy, NY 12180, USA. E-mail: mingmafudan@gmail.com
[b]School of Semiconductor and Chemical Engineering, Semiconductor Physics Research Center, Chonbuk National University, Jeonju 561-756, Korea. E-mail: cho.jaehee@gmail.com
[c]LED Business, Samsung Electronics, Yongin 446-920, Korea

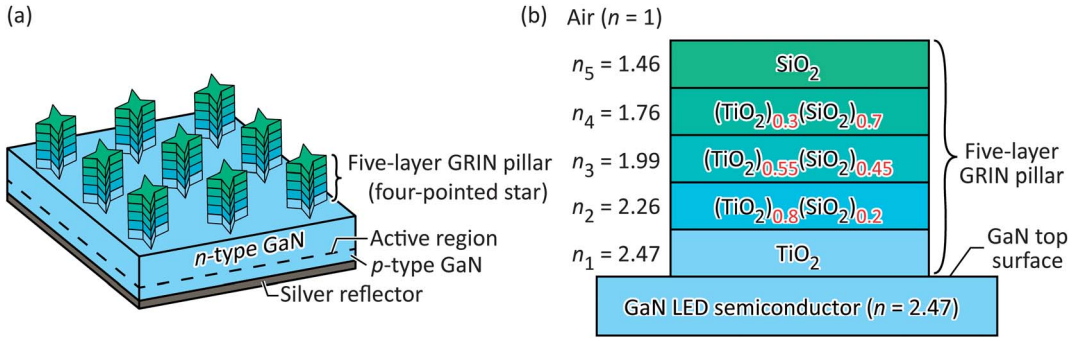

Fig. 1 Schematic diagrams of (a) a GRIN LED coated with an array of four-pointed-star-shaped GRIN micro-pillars and (b) the cross-section of a GRIN micro-pillar.

shown in Fig. 1b. By micro-patterning the GRIN coatings, light rays that would otherwise undergo total-internal-reflection will enter the GRIN micro-pillars. The graded-refractive-index profile of the micro-pillars will guide the light rays so that they strike the sidewalls of micro-pillars at near-normal incidence and are thus extracted out through the pillar sidewalls. In addition to an enhanced LEE of GaInN LEDs,[16] our results show that the GRIN micro-pillars can, at the same time, offer another advantage, *i.e.*, controllable emission patterns in GaInN LEDs. The structure of GRIN micro-pillars, including their planar geometric shape and size, will directly influence the emission pattern as well as the LEE. In this paper, we present GaInN LEDs having micro-patterned GRIN coatings. We show that the structure of the micro-pillars, including their planar geometric shape and size, can be varied to achieve (i) controllable emission patterns and (ii) a high LEE in GaInN LEDs.

2. Experimental section

Thin-film 1×1 mm^2 GaInN LEDs (nitrogen-face up) emitting at 445 nm are used as reference devices (planar LEDs). The crystallographically wet etched LEDs (surface-roughened LEDs) have a chemically roughened nitrogen-face (N-face) GaN surface, which is textured by using an aqueous 10% KOH (weight ratio) etching solution heated to 50 °C in which the samples are immersed for 4 min. To fabricate LEDs with patterned GRIN coatings (GRIN LEDs), a five-layer coating with varying compositions of TiO_2 and SiO_2 in each layer is deposited by co-sputtering on the non-roughened, smooth N-face GaN surface of thin-film LEDs. During the sputter deposition, the Ar flow rate and O_2 flow rate are 10 standard cubic centimeters per minute (sccm) and 0.5 sccm, respectively. The chamber pressure is kept at 2 mTorr. The substrate is kept at room temperature. The electrical powers applied to the two sputtering targets are carefully adjusted so that each layer has the desired refractive index. The refractive index and thickness of each layer are measured by VASE (Variable Angle Spectroscopic Ellipsometry). The total thickness of the GRIN coatings is around 1.5 μm, and the thickness of each layer is around 300 nm. Additionally, 130 nm of ITO is sputter-deposited on top of the GRIN coatings to serve as a hard etch mask for subsequent inductively coupled plasma (ICP) reactive ion etching (RIE). The ITO layer is then patterned by contact photolithography using Shipley Company's S1813 photoresist. After that, the ITO layer is etched using CH_4, H_2, and Cl_2 to form the ITO hard mask. The GRIN coatings are subsequently etched in a CHF_3 chemistry using the patterned ITO layer as a hard mask. After the removal of etch residues, GRIN micro-pillars with various planar geometric shapes and sizes are fabricated on the N-face GaN surface of a thin-film LED. The light-output power and the emission pattern of the LED chips are measured using a blue-enhanced Si PIN photo-detector positioned on a rotating arm, similar to a goniometer.

The refractive index and thickness of each layer are designed by ray-tracing simulation. The design rules of GRIN coatings for the purpose of eliminating total-internal-reflection at the semiconductor–air interface are as follows: for an m-layer GRIN coating with the first layer in contact with the LED top surface and the m^{th} layer in contact with air, the refractive index and thickness of each layer, from the first layer to the $(m-1)^{th}$ layer, are designed so that light rays entering each layer are either (i) escaping through the sidewall of this layer or (ii) entering the layer above. The refractive index and thickness of the last layer

Table 1 Designed and measured refractive index and thickness of each layer of a five-layer GRIN coating

	Refractive index n		Thickness (nm)		Measured extinction coefficient from 435 nm to 455 nm
	Measured	Designed	Measured	Designed	
Layer 1	2.46	2.47	330	300	0
Layer 2	2.23	2.26	326	300	0
Layer 3	1.98	1.99	309	300	0
Layer 4	1.77	1.76	302	300	0
Layer 5	1.47	1.46	295	300	0

(m^{th} layer) are designed so that all light rays entering this layer are extracted from either the sidewall or the top surface of this layer. The designed refractive indices for each layer of a five-layer GRIN coating are shown in Table 1. In our experiments, TiO_2 is selected since it is refractive-index-matched to GaN at the wavelength of 445 nm, so that there is a minimal out-coupling loss (Fresnel reflection loss). SiO_2 is selected since it is refractive-index-matched to the designed value of the top layer at a wavelength of 445 nm. The designed thickness is selected to be 300 nm so that (i) the thickness of each layer is greater than the effective wavelength of interest so that the behaviour of light in GRIN coatings can still be described using ray optics; and (ii) the total thickness of the GRIN coating is practical for thin-film deposition. The measured results are very close to the designed values, as shown in Table 1. The extinction coefficient of each layer of the five-layer GRIN coating is measured to be zero from 435 nm to 455 nm. Thus the GRIN coatings are measured to be virtually non-absorbing from 435 nm to 455 nm.

Fig. 2a–d show the top-view scanning electron micrographs of an array of circle-, square-, equilateral-triangle-, and four-pointed-star-shaped GRIN micro-pillars fabricated on the N-face GaN surface of a thin-film GaInN LED. Fig. 2e shows a cross-sectional scanning electron micrograph of five-layer GRIN layers on the N-face GaN surface of a thin-film GaInN LED. The GRIN micro-pillars are arranged in a rectangular pattern. The size of a GRIN micro-pillar is defined as the diameter of an equal-area circle. For example, the size of a four-pointed-star-shaped GRIN micro-pillar is 6 μm if the area of that four-pointed-star equals a circle with a diameter of 6 μm. For each planar geometric shape, GRIN micro-pillars with three sizes (8 μm, 6 μm, and 4 μm) are fabricated. The spacing between neighbouring GRIN micro-pillars is kept the same as its size, *i.e.*, the spacing between GRIN micro-pillars with a size of 6 μm is also 6 μm.

3. Results and discussion

3.1. GRIN LEDs for control of emission pattern

The planar reference LED and the surface-roughened LED have a Lambertian emission pattern with the peak emission intensity at the LED top-surface-normal. In contrast, the GRIN LED has a bidirectional emission pattern with intensity peaks at off-surface-normal directions. This is a confirmation of light extracted through the pillar sidewalls. Thus, in order to control the emission pattern of a GRIN LED, it is important to study the emission pattern from the sidewalls of GRIN pillars. Fig. 3 shows a schematic diagram illustrating ranges of angles of light rays extracted from the sidewalls of a GRIN pillar, where θ_1 to θ_5 represent the ranges of angles of light rays extracted from the bottom layer to the top layer of a GRIN micro-pillar, respectively. For example, for an array of circle-shaped GRIN micro-pillars with a pillar-height of 1.5 μm, a pillar-diameter of 4 μm, and spacing between neighboring pillars of 4 μm, the values of θ_1 to θ_5 are 71°, 75°, 79°, 84°, and 88°, respectively. A larger angle means that there can be extracted light rays that are further away from the LED top-surface-normal. There are two facts that we can learn from Fig. 3: firstly, the values of θ_1 to θ_5 depend on the structure of GRIN micro-pillars. For micro-pillars with a fixed height, a larger spacing between the neighboring pillars will cause larger values of θ_1 to θ_5, *i.e.*, the peak emission intensity will be at an angle that is further away from the LED top-surface-normal. Conversely, a smaller spacing between the neighboring pillars will cause the peak emission intensity to be at an angle that is closer to the LED top-surface-normal. Secondly, the value of θ is decreasing from θ_5 (top layer) to θ_1 (bottom layer). Thus, if more light rays are extracted from the upper layers of the GRIN micro-pillars, the peak emission intensity will be at an angle that is further away from the LED top-surface-normal. If more light rays are extracted from the lower layers of GRIN micro-pillars, then the peak emission

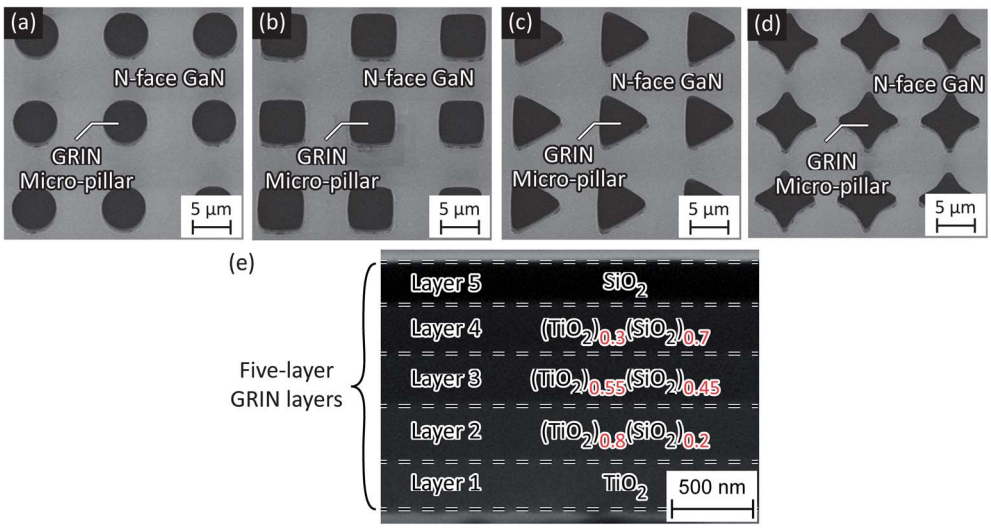

Fig. 2 Top-view scanning electron micrographs of an array of (a) circle-, (b) square-, (c) equilateral-triangle-, and (d) four-pointed-star-shaped GRIN micro-pillars fabricated on the nitrogen-face GaN surface of a thin-film GaInN LED. (e) Cross-sectional scanning electron micrograph of five-layer GRIN layers on the nitrogen-face GaN surface of a thin-film GaInN LED.

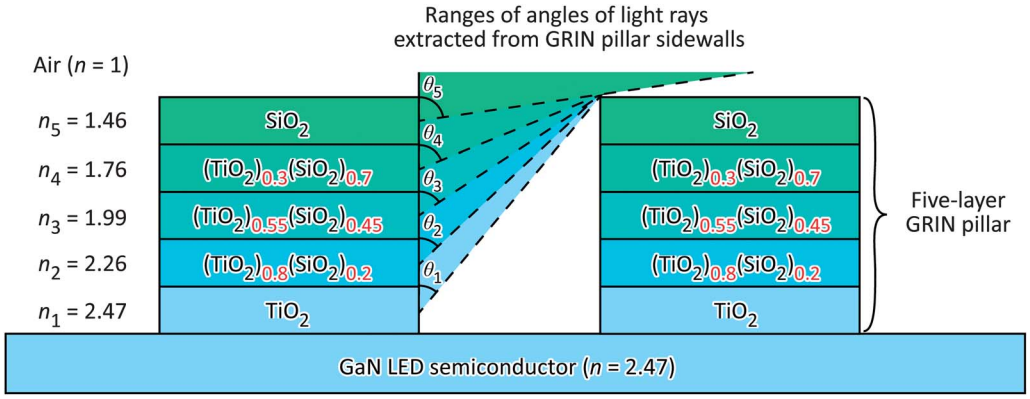

Fig. 3 Schematic diagram of ranges of angles of light rays extracted from the sidewalls of a GRIN pillar.

intensity will be at an angle that is closer to the LED top-surface-normal. These two facts can be used as guidance to design GRIN LEDs with controllable emission patterns.

Fig. 4a–d show the emission patterns of GRIN LEDs with peak emission intensities (θ_p) at $\pm 20^\circ$ to $\pm 50^\circ$ off-surface-normal. The emission pattern is symmetrical around the axis normal to the LED surface. As shown in Fig. 4, the emission pattern of GRIN LEDs can be controlled by varying the structures of GRIN micro-pillars, *i.e.*, their planar geometric shapes, sizes, and spacing. For example, for LEDs coated with GRIN micro-pillars with a given planar geometric shape, a larger spacing between pillars will have fewer light rays re-entering neighboring pillars, thus resulting in a stronger off-surface-normal emission, *i.e.*, an emission pattern with a larger θ_p. This contention is confirmed by comparing Fig. 4b with Fig. 4c. For LEDs coated with GRIN micro-pillars with a given pillar size and spacing, GRIN micro-pillars with angular shapes with acute angles, such as four-pointed-star-shaped GRIN micro-pillars, will have less trapped light rays than circle-shaped GRIN micro-pillars that are highly symmetrical.[17] (This will be explained in more detail in the next section, Section 3.2.) Thus, more light rays will be extracted from the lower layers of GRIN micro-pillars with angular shapes, *i.e.*, pillar shapes having

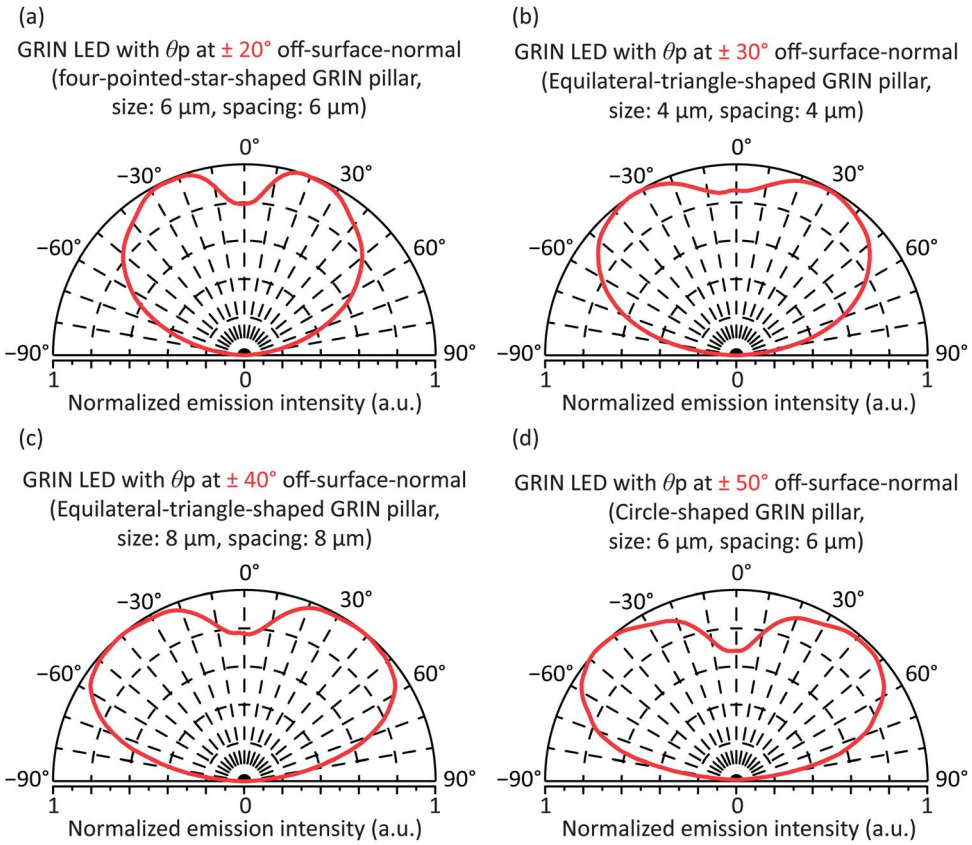

Fig. 4 Emission pattern of GRIN LEDs with peak emission intensities (θ_p) at (a) $\pm 20^\circ$, (b) $\pm 30^\circ$, (c) $\pm 40^\circ$, and (d) $\pm 50^\circ$ off-surface-normal.

acute-angle features. As can be learned from Fig. 3, if more light rays are extracted from the lower layers of GRIN micro-pillars, then the peak emission intensity will be at an angle that is closer to the LED top-surface-normal, *i.e.* a smaller θ_p. Thus, LEDs coated with GRIN micro-pillars with angular shapes will result in an emission pattern with a smaller θ_p, as can be confirmed by comparing Fig. 4a with Fig. 4d. This shows that by carefully designing a combination of the planar geometric shapes, sizes, and spacing of GRIN micro-pillars, we can control the emission pattern of LEDs, increase the light emission in certain desired directions, and thus eliminate the need for secondary optics on LEDs. Such secondary optics is bulky and has additional Fresnel losses.

3.2. GRIN LEDs for light-extraction efficiency enhancement

Fig. 5a shows the measured light-output power (LOP) as a function of the size of GRIN micro-pillars with various planar geometric shapes. For each data point shown in Fig. 5a, there are at least three samples measured and the average value is shown in Fig. 5a. The difference in the measured results is less than 5% for each data point. As shown in Fig. 5a, for LEDs coated with GRIN micro-pillars with a given planar geometric shape, the LOP increases as the size of GRIN micro-pillars decreases. This is because, given that the height of GRIN micro-pillars unchanged (1.5 μm), as the size of GRIN micro-pillars decreases, the ratio of the area of pillar sidewalls to the total surface area (sum of areas of pillar sidewall plus pillar top surfaces) increases. For example, for a circle-shaped pillar with a pillar radius r and a fixed pillar height h, the ratio of the area of pillar sidewalls to the total surface area is given by: $(2\pi rh)/(\pi r^2 + 2\pi rh) = (2h)/(r + 2h)$, which increases as r decreases. Since the sidewalls of GRIN micro-pillars are much more effective in extracting trapped light rays than their top surfaces, the LOP will increase as the ratio of the area of pillar sidewalls to the total surface area increases.

Also shown in Fig. 5a is the comparison among LEDs patterned with GRIN micro-pillars with various planar geometric shapes. LEDs patterned with an array of four-pointed-star-shaped and equilateral-triangle-shaped GRIN micro-pillars show a higher LOP than LEDs patterned with an array of square-shaped and circle-shaped GRIN micro-pillars. This is because although the GRIN micro-pillars are designed to eliminate total-internal-reflection in the cross-sectional plane normal to the semiconductor surface plane, light rays can continue to be trapped in the plane parallel to the semiconductor surface plane. For example, light rays inside a circle-shaped GRIN micro-pillar can propagate along the circumference of the pillar sidewalls and remain trapped. These trapped optical modes, often referred to as the whispering-gallery optical modes,[17] are more likely to exist in pillars with highly symmetric planar geometric shapes, such as circle-shaped pillars or square-shaped pillars. However, when the pattern contains angular shapes with no right angles and preferably acute angles, such as equilateral-triangle-shaped pillars and four-pointed-star-shaped pillars, the occurrence of whispering-gallery modes strongly diminishes. In addition, light rays will undergo multiple reflections when propagating towards the vertex of the angle with a progressively decreasing angle of incidence at the semiconductor–air interface. Thus, light rays guided by an acute angle will eventually have near-normal incidence and escape from the angle (*i.e.*, the GRIN micro-pillar) into the surrounding material. As a result, LEDs patterned with an array of four-pointed-star-shaped and equilateral-triangle-shaped GRIN micro-pillars show higher LOP than LEDs patterned with an array of square-shaped and circle-shaped GRIN micro-pillars.

There could be an overall uncertainty in the measured results as shown in Fig. 5(a). The overall uncertainty is due to fabrication imperfections such as (i) the sidewall-surface-roughness of the fabricated GRIN micro-pillars introduced by the dry etching; and (ii) the rounded corners resulting from the contact photolithography, *e.g.*, the rounded corners of the fabricated square-shaped GRIN micro-pillars as shown in Fig. 2(b).

Fig. 5b compares the emission intensity of (i) a planar reference LED, (ii) a surface-roughened LED, and (iii) a GRIN LED patterned with an array of four-pointed-star-shaped GRIN micro-pillars with a pillar-size of 4 μm and spacing between neighboring pillars of 4 μm. The GRIN LED shows a 155% enhancement in LOP over the planar reference LED; while the surface-roughened LED shows a 124% enhancement in LOP over the planar reference LED.

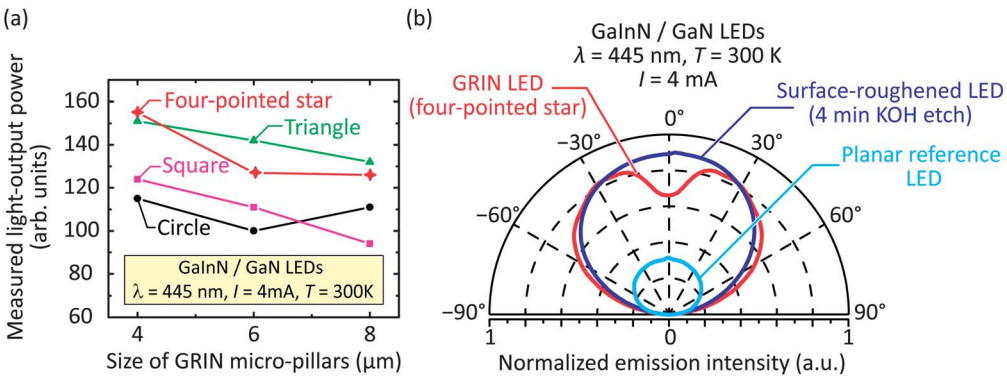

Fig. 5 (a) Measured light-output power as a function of the size of GRIN micro-pillars with various planar geometric shapes. (b) Measured emission intensity of a planar reference LED, a surface-roughened LED, and a GRIN LED patterned with an array of four-pointed-star-shaped GRIN micro-pillars with a pillar-size of 4 μm and spacing between neighboring pillars of 4 μm. The measured light-output power is calculated after integration over all angles in the three-dimensional space.

4. Conclusion

The unrestricted control of the surface structure and refractive index would allow for new and improved functionalities in opto-electronic devices. Specifically, micro-patterned GRIN coatings can enable control of emission pattern and promote light extraction in GaInN LEDs. We design and demonstrate coatings that are patterned into arrays of GRIN micro-pillars, each composed of five dielectric layers of $(TiO_2)_x(SiO_2)_{1-x}$ with the bottom layer (adjacent to semiconductor) having the highest refractive index and the top layer (adjacent to air) having the lowest one. The GRIN micro-pillars, including their planar geometric shape and size, are structured for emission pattern control and maximum LEE. It is shown that the peak emission intensity of the GRIN LEDs is controllable from $\pm 20^\circ$ to $\pm 50^\circ$ off the surface-normal. In addition, LEDs patterned with an array of four-pointed-star-shaped GRIN micro-pillars with a pillar-size of 4 μm and spacing between neighboring pillars of 4 μm show a 155% enhancement in LOP over an uncoated planar reference LED, showing great promise for GRIN LEDs to have emission-pattern control and high LEE. These two characteristics can be tuned to match specific target applications of the LEDs.[18]

Acknowledgements

The authors gratefully acknowledge support by Samsung Electronics, the National Science Foundation, Sandia National Laboratories, Department of Energy, and Applied Materials – Varian Semiconductor Business Unit. Author J. Cho gratefully acknowledges support by the Priority Research Centers Program (2009-0094031) and Basic Research Laboratory Program (2011-0027956) through the National Research Foundation of Korea funded by the Ministry of Education, Science and Technology.

Notes and references

1 M. R. Krames, O. B. Shchekin, R. Mueller-Mach, G. O. Mueller, L. Zhou, G. Harbers and M. G. Craford, *J. Disp. Technol.*, 2007, **3**, 160–175.
2 N. Horiuchi, *Nat. Photonics*, 2010, **4**, 738.
3 J. K. Kim and E. F. Schubert, *Opt. Express*, 2008, **16**, 21835–21842.
4 I. Moreno and C.-C. Sun, *Opt. Express*, 2008, **16**, 1808–1819.
5 M. Ma, A. N. Noemaun, J. Cho, E. F. Schubert, G. B. Kim and C. Sone, *Opt. Express*, 2012, **20**, 16677–16683.
6 T. X. Lee, C. Y. Lin, S. H. Ma and C. C. Sun, *Opt. Express*, 2005, **13**, 4175–4179.
7 M. Ma, F. W. Mont, X. Yan, J. Cho, E. F. Schubert, G. B. Kim and C. Sone, *Opt. Express*, 2011, **19**, A1135–A1140.
8 X. Long, R. Liao and J. Zhou, *IET Optoelectron.*, 2009, **3**, 40–46.
9 E. F. Schubert, *Light Emitting Diodes*, Cambridge University Press, Cambridge, UK, 2nd edn, 2006.
10 J. Jiang, S. To, W. B. Lee and B. Cheung, *Optik*, 2010, **121**, 1761–1765.
11 K. Wang, S. Liu, F. Chen, Z. Qin, Z. Liu and X. Luo, *J. Opt. A: Pure Appl. Opt.*, 2009, **11**, 105501.
12 K. Wang, S. Liu, F. Chen, Z. Qin, Z. Liu and X. Luo, *Opt. Express*, 2010, **18**, 413–425.
13 T. Fujii, Y. Gao, R. Sharma, E. L. Hu, S. P. Denbaars and S. Nakamura, *Appl. Phys. Lett.*, 2004, **84**, 855–857.
14 D. A. Stocker, E. F. Schubert and J. M. Redwing, *Appl. Phys. Lett.*, 1998, **73**, 2654–2656.
15 C.-F. Lin, J.-J. Dai, Z.-J. Yang, J.-H. Zheng and S.-Y. Chang, *Electrochem. Solid-State Lett.*, 2005, **8**, C185–C188.
16 F. W. Mont, A. J. Fischer, A. N. Noemaun, D. J. Poxson, J. Cho, E. F. Schubert, M. H. Crawford, D. D. Koleske and K. W. Fullmer, *Phys. Status Solidi A*, 2012, **209**, 2277–2280.
17 H. Luo, J. K. Kim, Y. A. Xi, E. F. Schubert, J. Cho, C. Sone and Y. Park, *Appl. Phys. Lett.*, 2006, **89**, 041125.
18 M. Ma, J. Cho, E. F. Schubert, G. B. Kim and C. Sone, *SPIE Newsroom*, 2013, DOI: 10.1117/2.1201305.004900.

